Space Physics Seminar, 2 July 2014

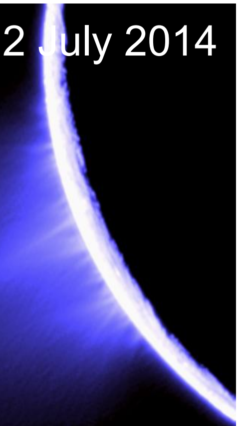

# Dust-plasma interaction in Saturn's inner magnetosphere and its magnetosphere-ionosphere coupling


Shotaro Sakai

*Department of Physics and Astronomy, University of Kansas*

Collaborators:

S. Watanabe[1], M. W. Morooka[2], M. K. G. Holmberg[3,4], J. –E. Wahlund[3], D. A. Gurnett[5], W. S. Kurth[5]

1: *Department of Systems and Informatics, Hokkaido Information University*

2: *LASP, University of Colorado at Boulder*

3: *Swedish Institute of Space Physics, Uppsala*

*4: Department of Astronomy and Physics, Uppsala University*

*5: Department of Astronomy and Physics, The University of Iowa*


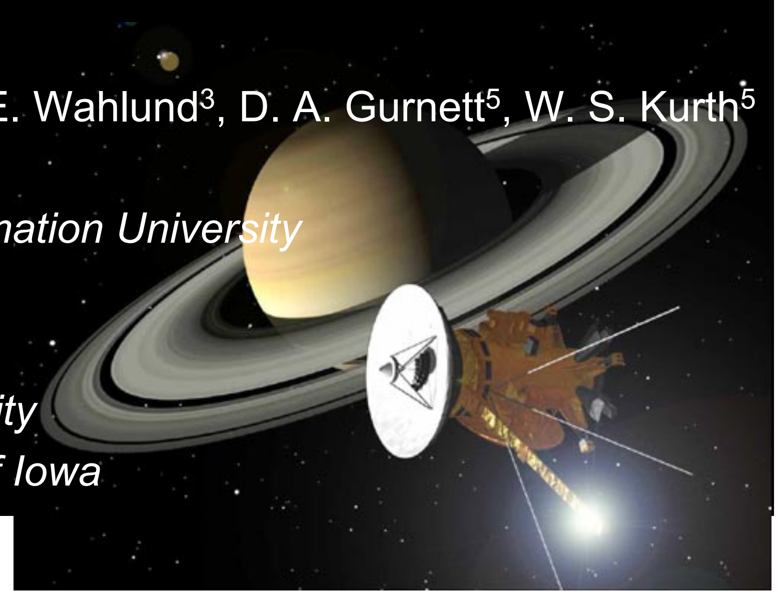

# Outline

1. Modeling of the inner magnetosphere
    - Based on Sakai et al. [2013]
2. Modeling of the ionosphere
3. Magnetosphere-ionosphere coupling
4. Summary

# Introduction

# Enceladus plume & E ring

- Enceladus plume (~3.95 Rs)
  - Water gas
- E ring
  - 3 – 8 Rs
  - Water group ion
  - Dust
  - Source: Mainly Enceladus plume
  - Kepler motion

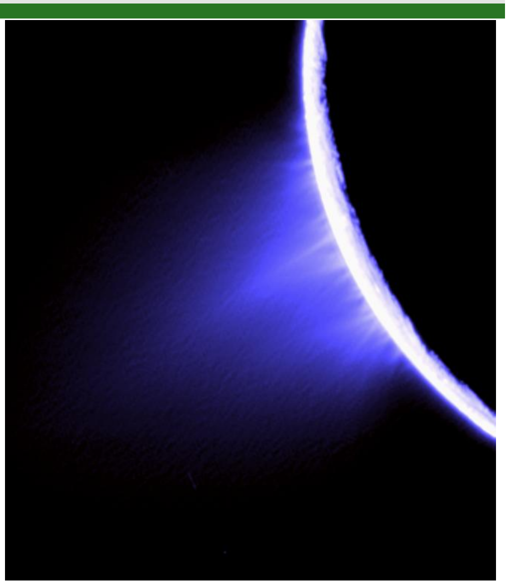

Enceladus & E ring [*NASA/JPL*]

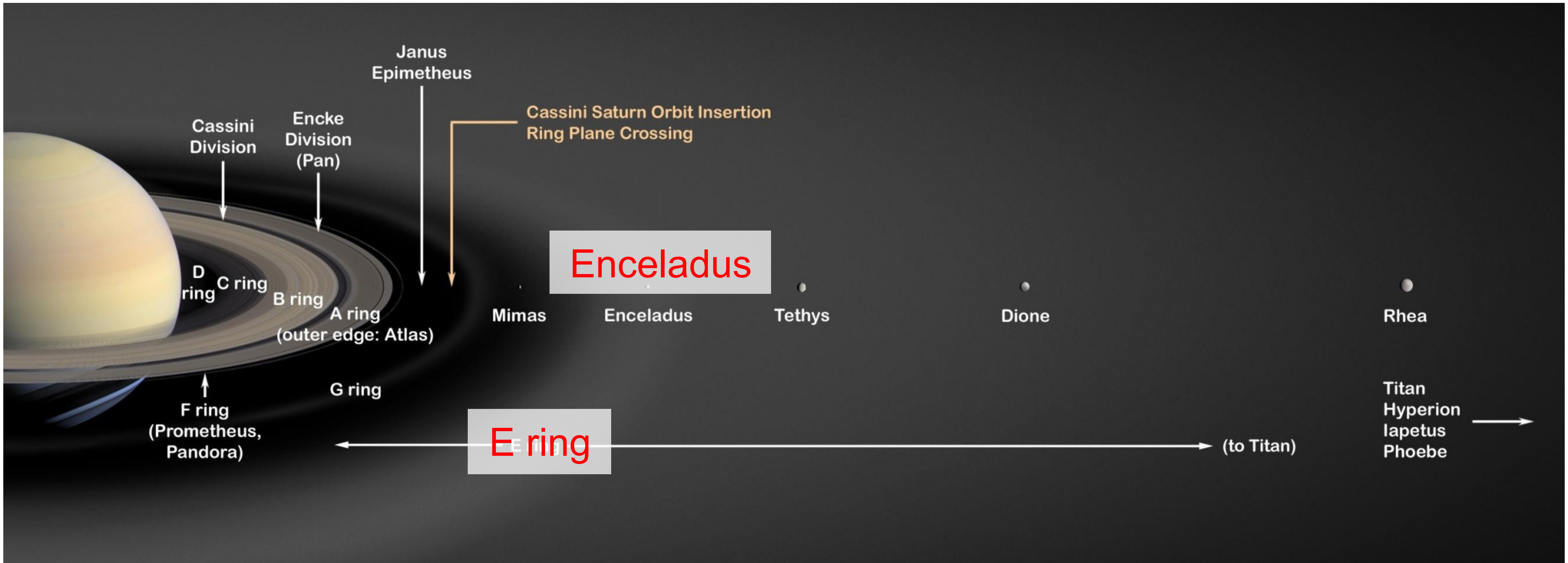

# Co-rotation deviation by dusts?

- Ion observations from the Cassini RPWS/LP in Saturn's magnetosphere
  - Ion has slower speed than the co-rotation [*Wahlund et al.*, 2009; *Morooka et al.*, 2011; *Holmberg et al.*, 2012].

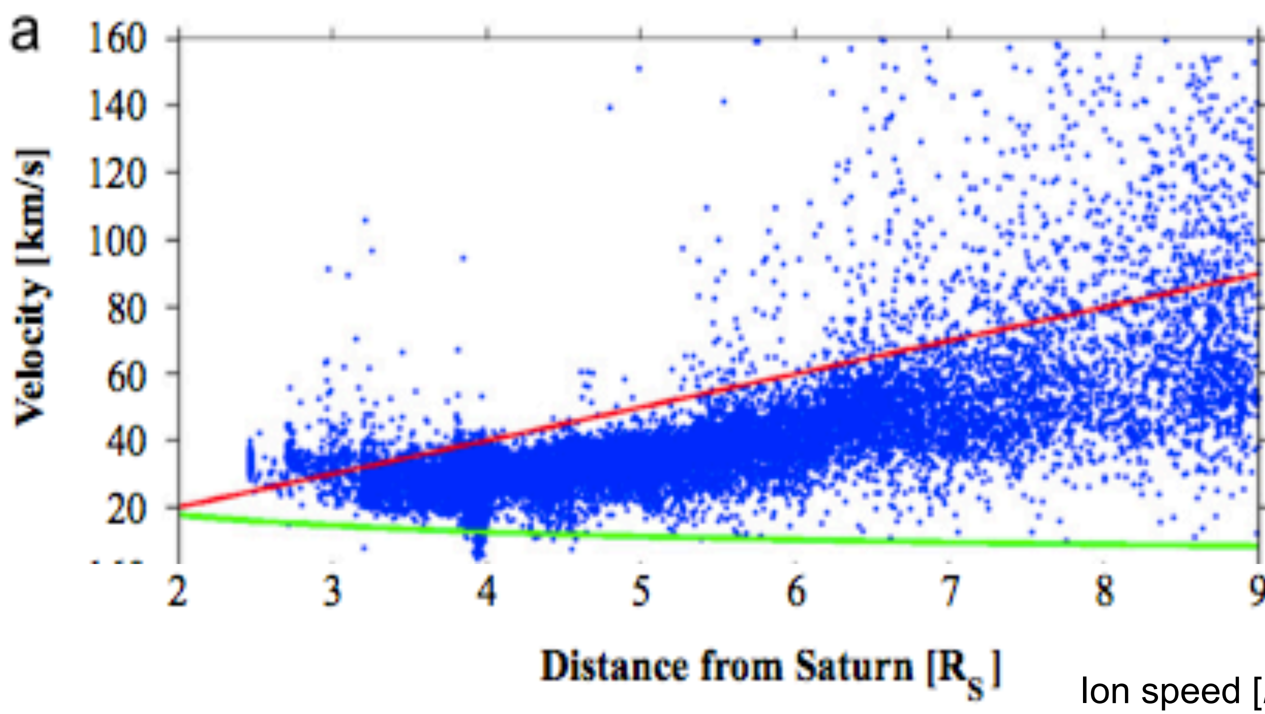


Ion speed [*Holmberg et al.*, 2012]

# Co-rotation deviation by dusts?

- Ion observations from the Cassini RPWS/LP in Saturn's magnetosphere
  - Ion has slower speed than the co-rotation [*Wahlund et al.*, 2009; *Morooka et al.*, 2011; *Holmberg et al.*, 2012].
    - Do dusts affect the ion velocities in the inner magnetosphere?

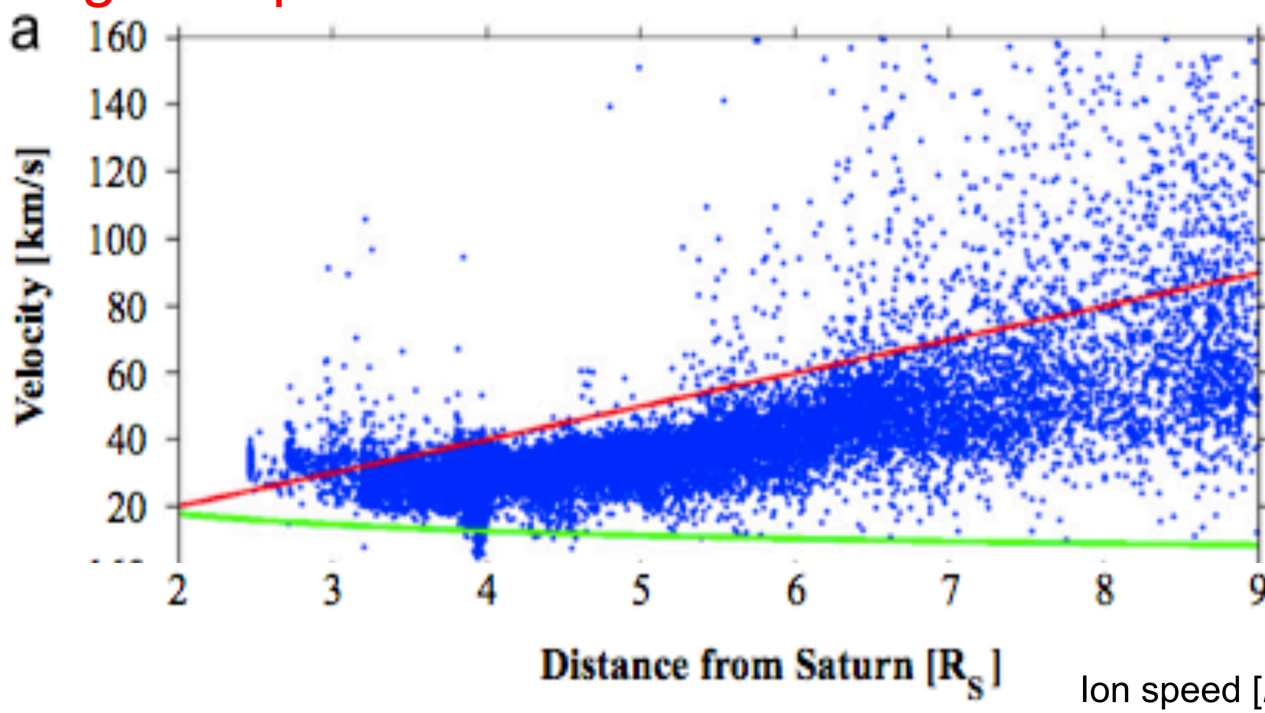


Ion speed [*Holmberg et al.*, 2012]

# Purpose of this thesis

- Investigation of dust-plasma interaction and magnetosphere-ionosphere coupling in the Saturn's inner magnetosphere

- Understanding of generation process for magnetospheric current, electric field and ion-dust collision

- Understanding of relationship of ionospheric conductivity with the magnetospheric ion speed

# Plasma in the plume

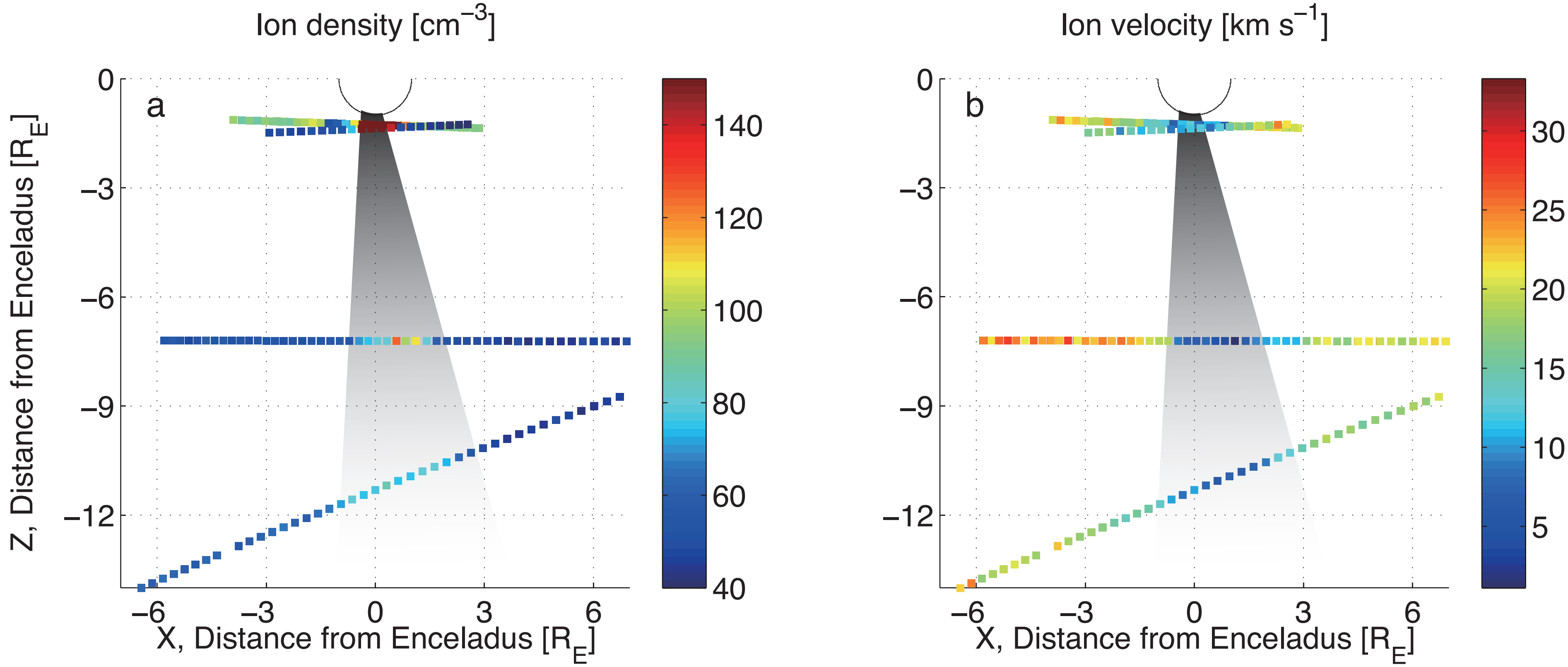


- Density
  - $N_e/N_i < 0.01$ at 1.3 $R_E$
    ~ 0.7 at 11 $R_E$
- Ion speed
  - $V_i \sim V_{Kepler}$

Ion density and speed in plume [*Sakai et al.*, in prep.]

## Modeling of the inner magnetosphere

# Model

- Multi-fluid model ($H^+$, $H_2O^+$, dust, $e^-$)
- 1 dimension (radial direction), 2 $R_S$ to 10 $R_S$
  - $V_r$, $V_\phi$ are calculated.

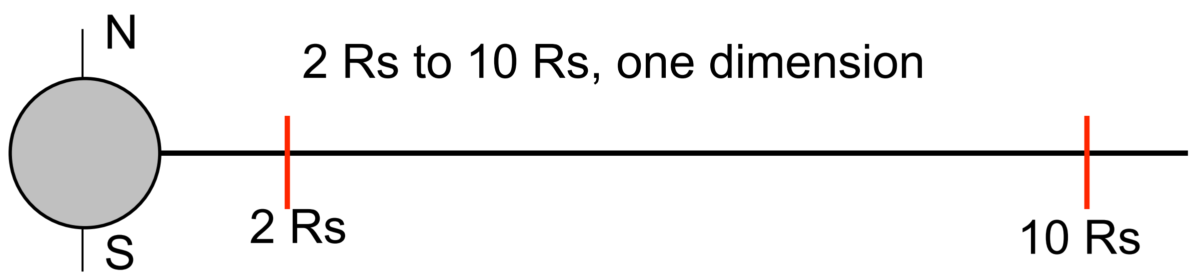


- Initial condition
  - Ion speed: Co-rotation speed; Dust speed: Keplerian speed
- Boundary condition
  - Inner boundary
    - Ion speed: Co-rotation speed; Dust speed: Keplerian speed
  - Open outer boundary

# Inner magnetospheric model

- Momentum equations
  - $H^+$, $H_2O^+$, $e^-$ and dust

$$\rho_k \frac{\partial \mathbf{v}_k}{\partial t} + \rho_k (\mathbf{v}_k \cdot \nabla)\mathbf{v}_k = n_k q_k (\mathbf{E} + \mathbf{v}_k \times \mathbf{B}) - \nabla p_k - \rho_k \mathbf{g} + \sum_l \rho_k \nu_{kl} (\mathbf{v}_k - \mathbf{v}_l) - \sum_l S_{k,l} (\mathbf{v}_k - \mathbf{v}_l)$$

Chemical term

- Dust: $q_d = 4\pi\varepsilon_0 r_d \phi$
  - $r_d$ = 100 nm; $\phi$ = -2 V

| | |
|---|---|
| $S_k$ | Production rate |
| $n_k$ | Number density |
| $\mathbf{B}$ | Magnetic field |
| $q_d$ | Charge quantity of dust |
| $r_d$ | Dust radius |
| $\phi$ | Dust surface potential |
| $\varepsilon_0$ | Permittivity |

| | |
|---|---|
| $\mathbf{V}_k$ | Velocity |
| $\mathbf{E}$ | Electric field |
| $\mathbf{g}$ | Gravity |
| $\rho_k$ | Mass density |
| $p$ | Pressure |
| $e$ | Charge quantity |
| $\nu_{kl}$ | Collision frequency |

# Chemical reactions

- For ion production rate
  - Water group ion and $H^+$
  - 9 reactions

| Reactions | Rates [$m^3\ s^{-1}$] | References |
|---|---|---|
| $H^+ + H_2O \rightarrow H + H_2O^+$ | $2.60\times10^{-15}$ | *Burger et al.* [2007], *Lindsay et al.* [1997] |
| $O^+ + H_2O \rightarrow O + H_2O^+$ | $2.13\times10^{-15}$ | *Burger et al.* [2007], *Dressler et al.* [2006] |
| $H_2O^+ + H_2O \rightarrow H_2O + H_2O^+$ | $5.54\times10^{-16}$ | *Burger et al.* [2007], *Lishawa et al.* [1997] |
| $H_2O^+ + H_2O \rightarrow OH + H_3O^+$ | $3.97\times10^{-16}$ | *Burger et al.* [2007], *Lishawa et al.* [1997] |
| $OH^+ + H_2O \rightarrow OH + H_2O^+$ | $5.54\times10^{-16}$ | *Burger et al.* [2007], *Itikawa and Mason* [2005] |
| $H_2O + e \rightarrow H_2O^+ + 2e$ | | *Burger et al.* [2007], *Itikawa and Mason* [2005] |
| $H_2O + e \rightarrow OH^+ + H + 2e$ | $10^{-18}$ (total) | *Burger et al.* [2007], *Itikawa and Mason* [2005] |
| $H_2O + e \rightarrow O^+ + H_2 + 2e$ | | *Burger et al.* [2007], *Itikawa and Mason* [2005] |
| $H_2O + e \rightarrow H^+ + OH + 2e$ | $10^{-22}$ | *Burger et al.* [2007], *Itikawa and Mason* [2005] |

# Inner magnetospheric model

- Momentum equations
  - $H^+$, $H_2O^+$, $e^-$ and dust

$$\rho_k \frac{\partial \mathbf{v}_k}{\partial t} + \rho_k (\mathbf{v}_k \cdot \nabla)\mathbf{v}_k = n_k q_k (\mathbf{E} + \mathbf{v}_k \times \mathbf{B}) - \nabla p_k - \rho_k \mathbf{g} + \sum_l \rho_k \nu_{kl} (\mathbf{v}_k - \mathbf{v}_l) - \sum_l S_{k,l} (\mathbf{v}_k - \mathbf{v}_l)$$

Electric field — Collision term — Chemical term

- Dust: $q_d = 4\pi\varepsilon_0 r_d \phi$
  - $r_d$ = 100 nm; $\phi$ = -2 V

| | |
|---|---|
| $S_k$ | Production rate |
| $n_k$ | Number density |
| $\mathbf{B}$ | Magnetic field |
| $q_d$ | Charge quantity of dust |
| $r_d$ | Dust radius |
| $\phi$ | Dust surface potential |
| $\varepsilon_0$ | Permittivity |

| | |
|---|---|
| $\mathbf{V}_k$ | Velocity |
| $\mathbf{E}$ | Electric field |
| $\mathbf{g}$ | Gravity |
| $\rho_k$ | Mass density |
| $p$ | Pressure |
| $e$ | Charge quantity |
| $\nu_{kl}$ | Collision frequency |

# Electric field

- M-I coupling for deriving electric field, E

| | |
|---|---|
| $\mathbf{j}$ | Current density |
| $\mathbf{E}_{cor}$ | Co-rotational Electric field |
| $\Sigma_i$ | Ionospheric conductivity |
| $D$ | Thickness of dust |
| $v_{thk}$ | Thermal velocity |

$$\Sigma_i\left(\mathbf{E}_{cor} - \mathbf{E}\right) = \mathbf{j}D$$

$$\mathbf{j} = en_i\mathbf{v}_i - en_e\mathbf{v}_e - q_d n_d \mathbf{v}_d$$

↓ ↓ ↓

$$\mathbf{E} = \mathbf{E}_{cor} - \frac{\mathbf{j}D}{\Sigma_i}$$

Thickness of dust distribution

- Ionospheric conductivity $\Sigma_i$: 1 S

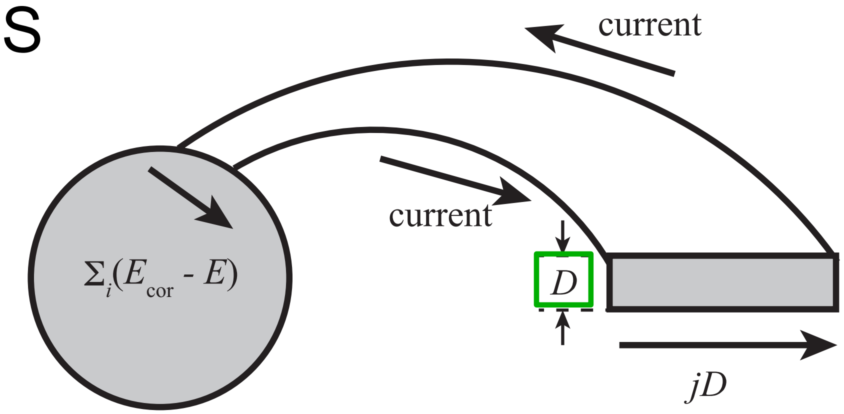

# Density profile & Thickness of dust

- 2 cases for dust density $N_d$

$$n_w = n_e + \frac{q_d}{e} n_d - n_p$$

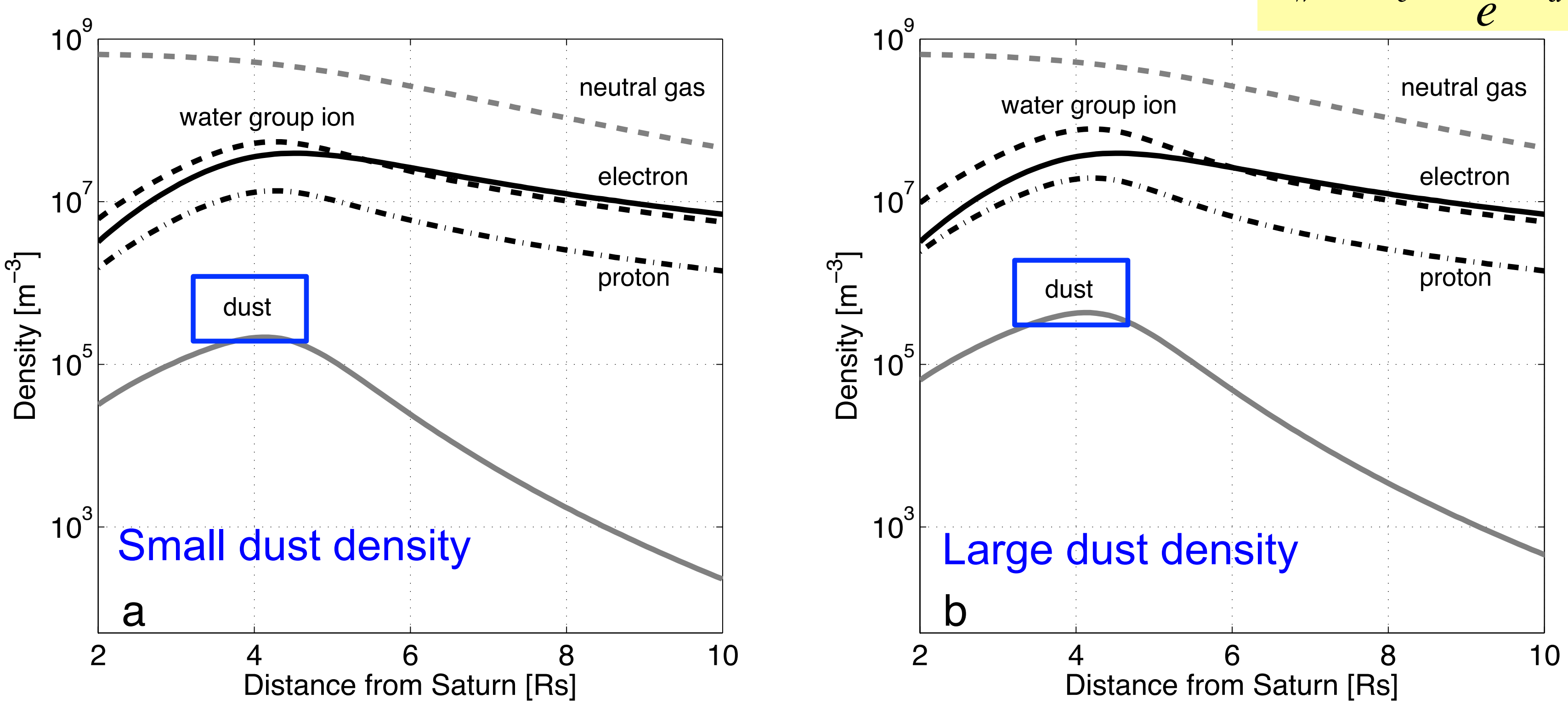


- 3 cases for thickness of dust distribution *D*
  1. $D = R_S$
  2. $D = 2\ R_S$
  3. $D = 3\ R_S$

# Results: Ion velocity

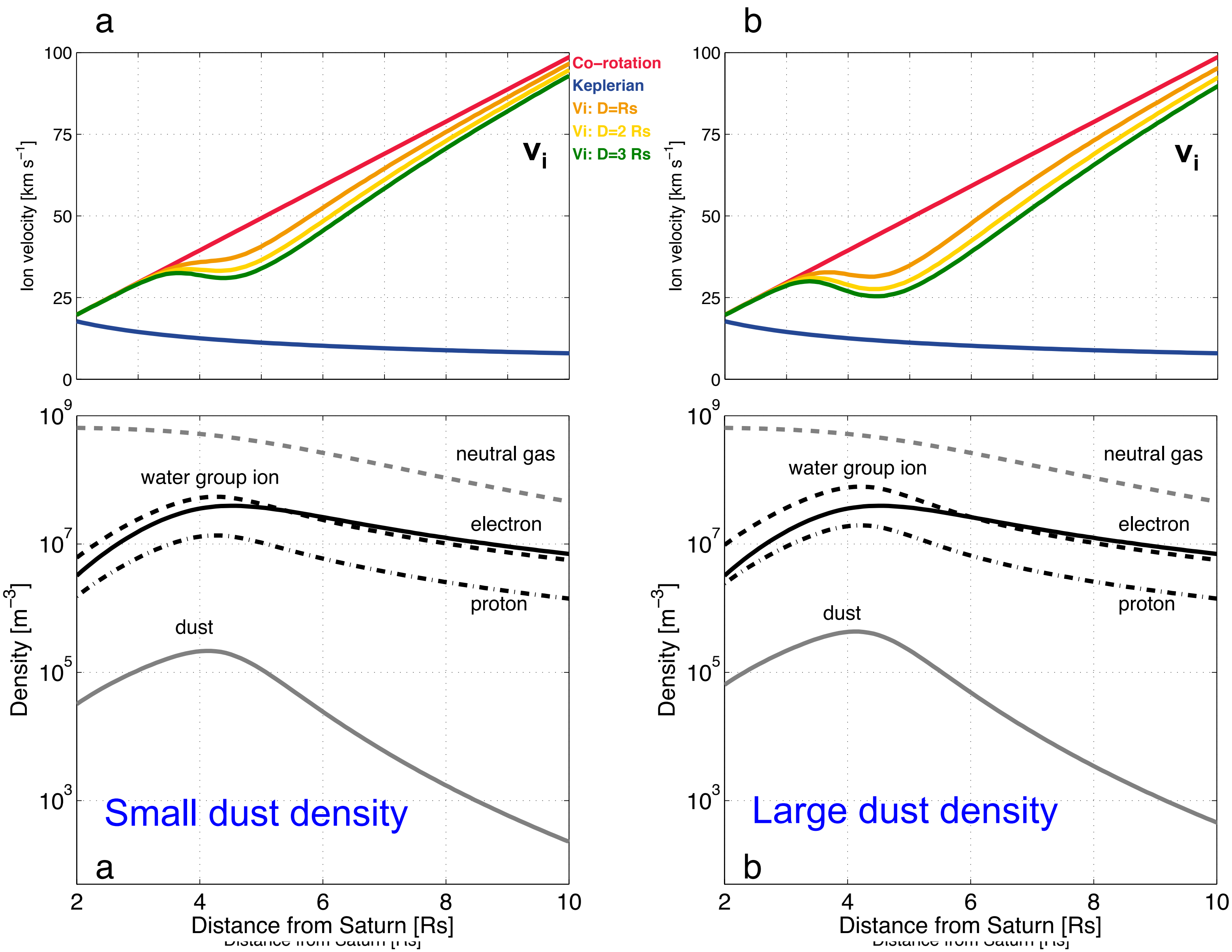

# Results: Ion velocity

$$\mathbf{E} = \mathbf{E}_{cor} - \frac{\mathbf{j}D}{\Sigma_i}$$

$$\mathbf{v}_i \approx \frac{\mathbf{E} \times \mathbf{B}}{B^2}$$

$$< \mathbf{v}_{cor}$$

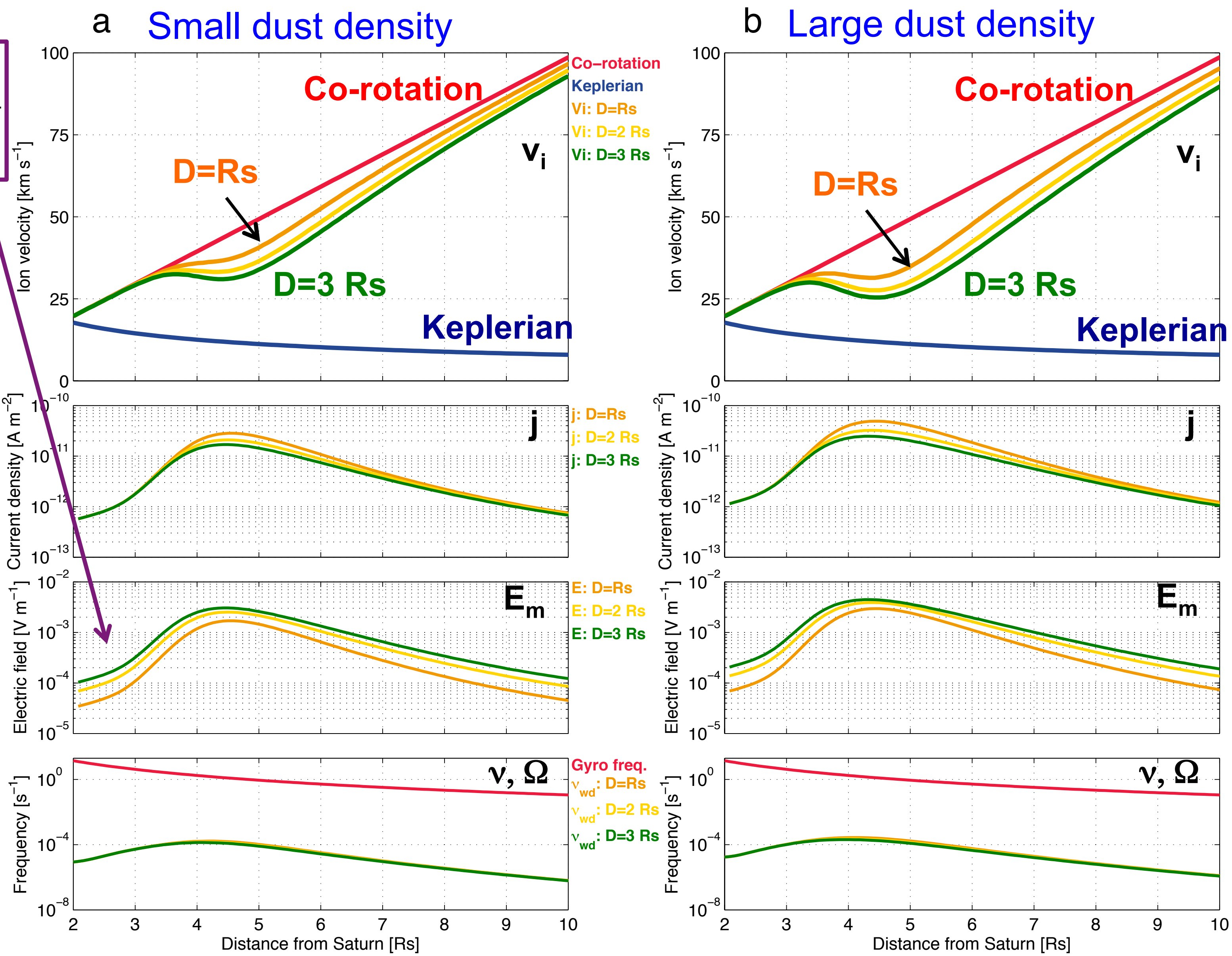

# Comparison with LP observation

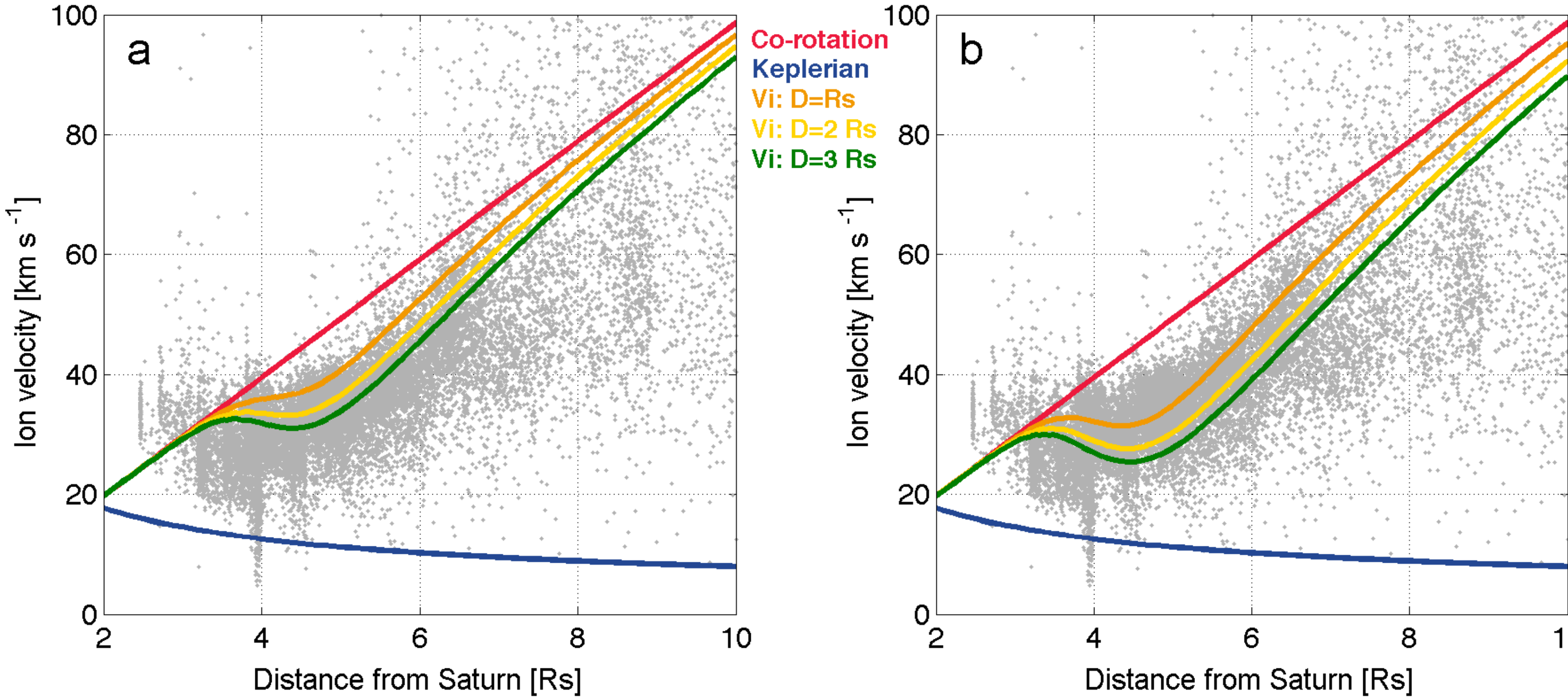


Small dust density

Large dust density

- Consistent with observations in $N_d > \sim 10^5\ m^{-3}$ and/or $D > 1\ R_S$.

# Comparison with LP observation

- Change $\Sigma_i$
  - 0.1 S
  - 1 S
  - 10 S

$$\Sigma_i(\mathbf{E}_{cor} - \mathbf{E}) = \mathbf{j}D$$

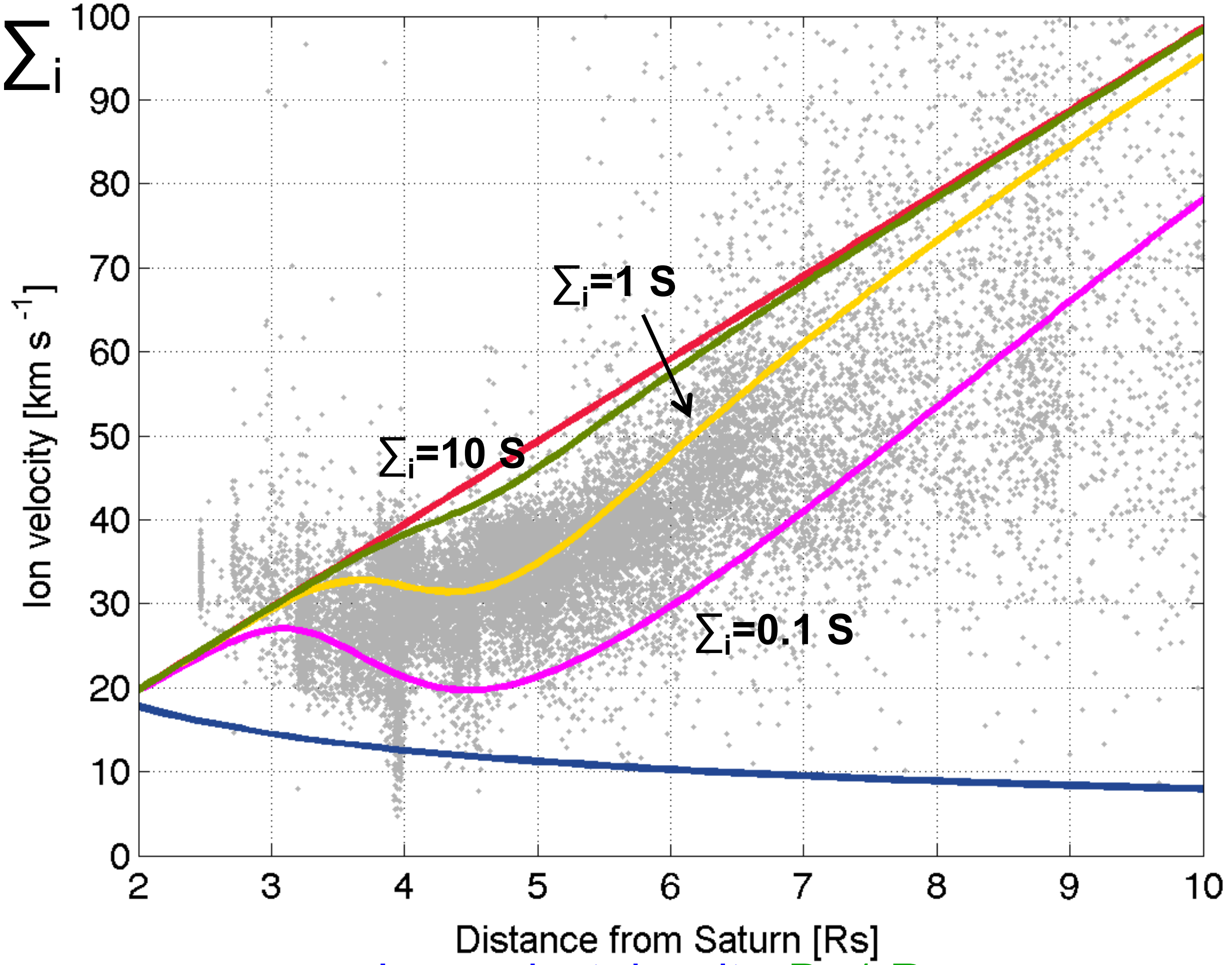


Large dust density, D=1 $R_S$

- $V_i$ is slower when $\Sigma_i$ is smaller.
- $V_i$ strongly depends on $\Sigma_i$.

# Summary of IM-modeling

- Co-rotation lag
  - Dust-plasma interaction
    - The dust–plasma interaction is significant when *D* is large and/or $N_d$ is high.
      - $N_{d\ max} > \sim 10^5\ m^{-3}$
      - $D > 1\ R_S$
    - The inner magnetospheric total current along a magnetic field line weakens E.
- Ionosphere and magnetosphere are strongly coupled.
  - $V_i$ depends on $\sum_i$.

# Modeling of the ionosphere & Magnetosphere-ionosphere coupling

# Co-rotation deviation by dusts?

- Ionospheric Pedersen conductivity
  - E depends on the conductivity.

$$\rho_k \frac{\partial \mathbf{v}_k}{\partial t} + \rho_k (\mathbf{v}_k \cdot \nabla) \mathbf{v}_k = n_k q_k (\mathbf{E} + \mathbf{v}_k \times \mathbf{B}) - \nabla p_k - \rho_k \mathbf{g} + \sum_l \rho_k \nu_{kl} (\mathbf{v}_k - \mathbf{v}_l) - \sum_l S_{k,l} (\mathbf{v}_k - \mathbf{v}_l)$$

Electric field

$$\Sigma_i (\mathbf{E}_{cor} - \mathbf{E}) = \mathbf{j} D$$

Pedersen conductivity

$$\sigma_p = \sum_i \frac{\nu_i}{\nu_{in}^2 + \omega_{ci}^2} \frac{n_i e^2}{m_i} + \frac{\nu_e}{\nu_{en}^2 + \omega_{ce}^2} \frac{n_e e^2}{m_e} \qquad \Sigma_i = \int_{z_1}^{z_2} \sigma_p ds$$

- However, it is one of the open questions.
  - ~0.1-100 S [*Connerney et al.*, 1983; *Cheng and Waite*, 1988]
  - ~0.02 S [*Saur et al.*, 2004]
  - 1--10 S [*Cowley et al.*, 2004; *Moore et al.*, 2010]
- We find the ionospheric $N_i$ for deriving $\sum_i$.

# Saturn’s ionosphere

- $N_e$ observation from Cassini occultations
  - $N_e$ (average between dusk and dawn)
    - Peak density: ~$10^{10}$ $m^{-3}$; Peak alt.: ~1200 km

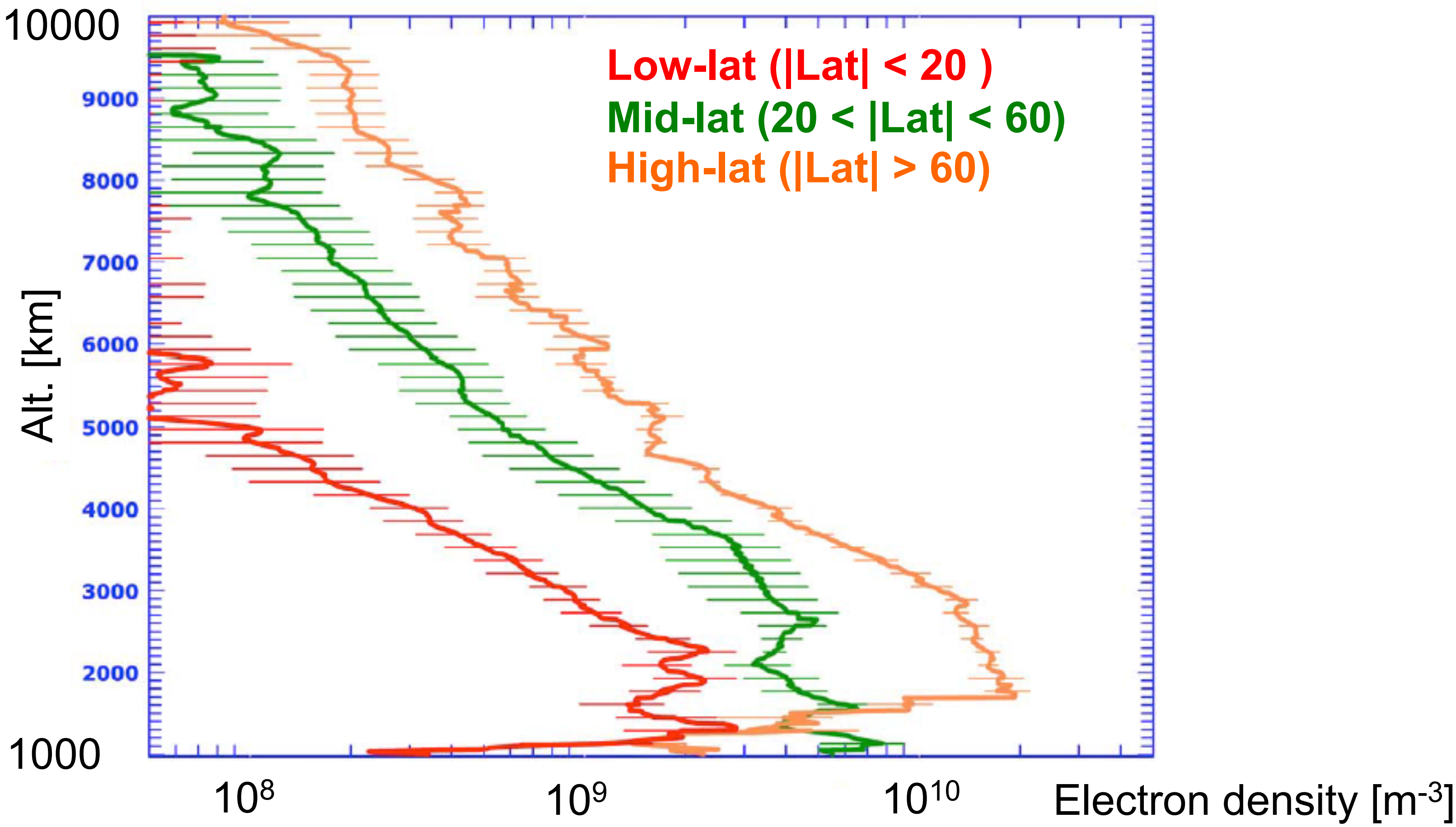


Electron density by occultations [*Kliore et al.*, 2009]

# Saturn's ionosphere

- Model [*Moore et al.* 2008]
  - $N_e$
    - Average peak density: $\sim 10^{10}$ $m^{-3}$
    - Peak alt.: ~1200 km
  - $T_e$
    - Max: 500 K
    - Alt.: > 1500 km
- But only below ~3000 km
  - How is the magnetospheric influence?

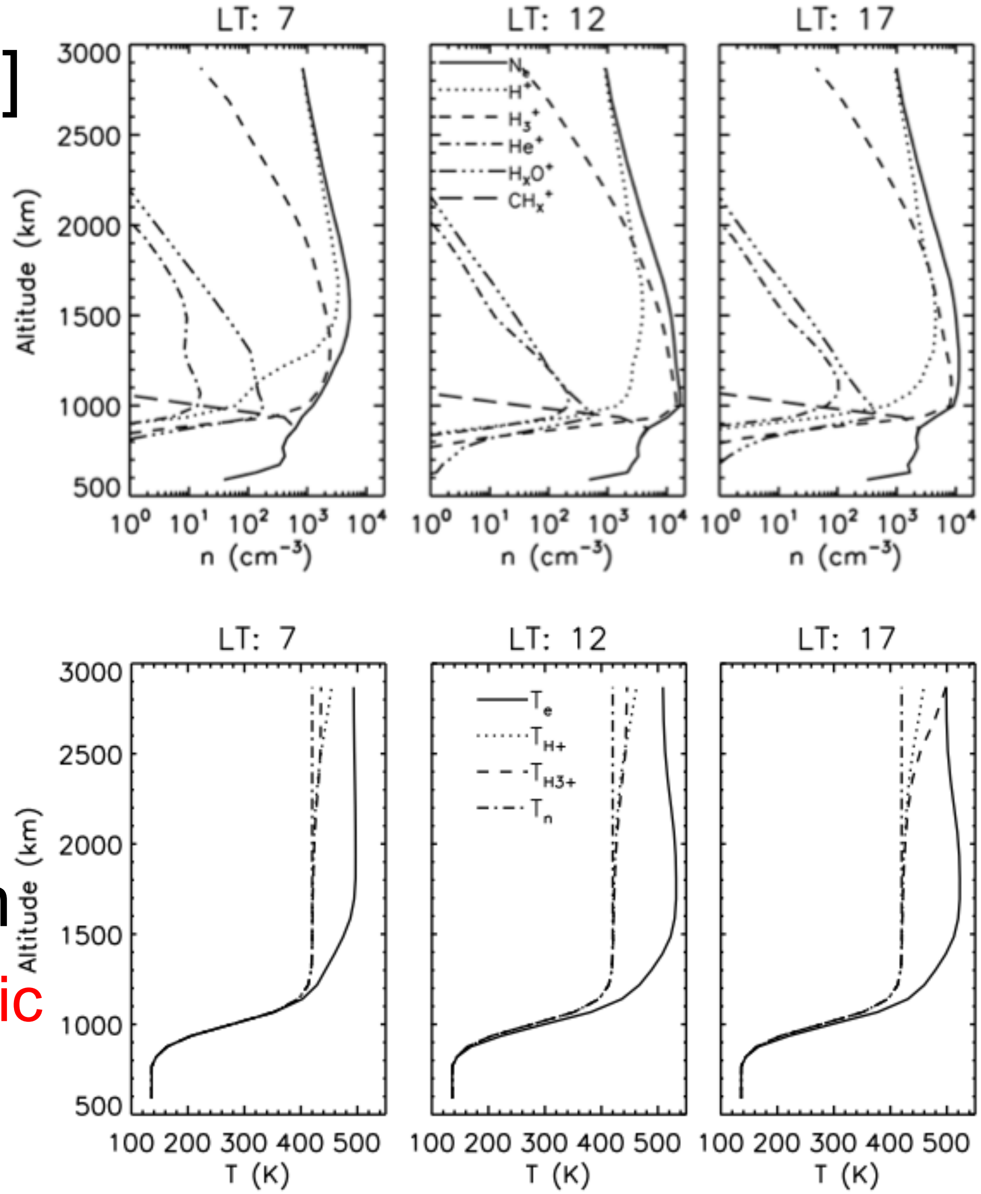


Plasma density and temperature by modeling [*Moore et al.*, 2008]

# Purpose

- Construction of an ionospheric model including the inner magnetosphere.
- Estimation of the ionospheric Pedersen conductivity from plasma density in the Saturn’s ionosphere
- Investigation of the influence of magnetosphere to ionosphere

# 3 dimensional ionospheric model

| | |
|---|---|
| $v_{\parallel}$ | Field-aligned Velocity |
| $E_{\parallel}$ | Electric field |
| $A$ | Magnetic flux cross-section |
| $g$ | Gravity and CF |
| $T$ | Temperature |
| $Q$ | Heating rate |
| $\kappa$ | Diffusion coefficient |

- Primitive equations
  - Ion

Density: $$\frac{\partial \rho_i}{\partial t} + \frac{1}{A}\frac{\partial\left(A\rho_i v_{i,\parallel}\right)}{\partial s} = S_i - L_i$$

Momentum: $$\rho_i \frac{\partial v_{i,\parallel}}{\partial t} + \rho_i v_{i,\parallel}\frac{\partial v_{i,\parallel}}{\partial s} = n_i e E_{\parallel} - \frac{\partial p_i}{\partial s} - \rho_i g - \sum_k \rho_i \nu_{ik}\left(v_{i,\parallel} - v_{k,\parallel}\right)$$

Temperature: $T_i = T_e$

$N_i$ ($H^+$, $H_2^+$, $H_3^+$, $He^+$, $H_2O^+$ and $H_3O^+$),

$V_i$ ($H^+$, $H_2^+$, $H_3^+$, $He^+$, [$H_2O^+$, $H_3O^+ = 0$]),

$T_e$, $T_i$

  - Electron

Density: $$n_e = \sum_i n_i$$

Momentum: $$E_{\parallel} = -\frac{1}{e n_e}\frac{\partial p_e}{\partial s}$$

Temperature: $$\frac{\partial T_e}{\partial t} - \frac{2}{3}\frac{1}{A}\frac{\partial}{\partial s}\left(A\kappa_e \frac{\partial T_e}{\partial s}\right) = Q_{EUV} + Q_{coll} + Q_{joule} + Q_{ph,ionos}$$

# Model

- Dipole coordinate system
  - Along the magnetic field line → 1 dimension

  \+ Increasing the number of magnetic field line → 2 dimensions

  \+ Time evolution → 3 dimensions

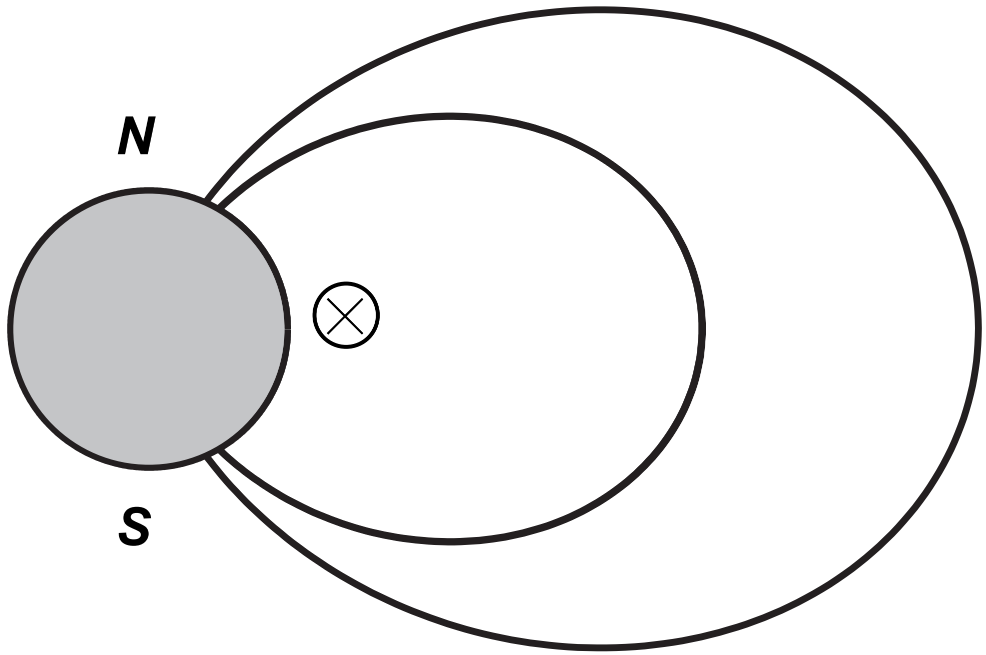

# 3 dimensional ionospheric model

- Primitive equations
  - Ion

Source and Loss rate

Density: $$\frac{\partial \rho_i}{\partial t} + \frac{1}{A}\frac{\partial\left(A\rho_i v_{i,\parallel}\right)}{\partial s} = \boxed{S_i - L_i}$$

Momentum: $$\rho_i \frac{\partial v_{i,\parallel}}{\partial t} + \rho_i v_{i,\parallel}\frac{\partial v_{i,\parallel}}{\partial s} = n_i e E_{\parallel} - \frac{\partial p_i}{\partial s} - \rho_i g - \sum_k \rho_i \nu_{ik}\left(v_{i,\parallel} - v_{k,\parallel}\right)$$

Temperature: $T_i = T_e$

| | |
|---|---|
| $v_{\parallel}$ | Field-aligned Velocity |
| $E_{\parallel}$ | Electric field |
| $A$ | Magnetic flux cross-section |
| $g$ | Gravity and CF |
| $T$ | Temperature |
| $Q$ | Heating rate |
| $\kappa$ | Diffusion coefficient |

$N_i$ ($H^+$, $H_2^+$, $H_3^+$, $He^+$, $H_2O^+$ and $H_3O^+$),

$V_i$ ($H^+$, $H_2^+$, $H_3^+$, $He^+$, [$H_2O^+$, $H_3O^+$ = 0]),

$T_e$, $T_i$

  - Electron

Density: $$n_e = \sum_i n_i$$

Momentum: $$E_{\parallel} = -\frac{1}{e n_e}\frac{\partial p_e}{\partial s}$$

Temperature: $$\frac{\partial T_e}{\partial t} - \frac{2}{3}\frac{1}{A}\frac{\partial}{\partial s}\left(A\kappa_e \frac{\partial T_e}{\partial s}\right) = Q_{EUV} + Q_{coll} + Q_{joule} + Q_{ph,ionos}$$

# Source & Loss

- Chemical reactions of 6 ion components
  - $H^+$, $H_2^+$, $H_3^+$, $He^+$, $H_2O^+$ and $H_3O^+$
  - 29 reactions

| Chemical reaction | Rate coefficiants | References |
|---|---|---|
| $H + h\nu \rightarrow H^+ + e^-$ | | *Moses and Bass* [2000] |
| $H_2 + h\nu \rightarrow H^+ + H + e^-$ | | *Moses and Bass* [2000] |
| $H_2 + h\nu \rightarrow H_2^+ + e^-$ | | *Moses and Bass* [2000] |
| $He + h\nu \rightarrow He^+ + e^-$ | | *Moses and Bass* [2000] |
| $H_2O + h\nu \rightarrow H^+ + OH + e^-$ | | *Moses and Bass* [2000] |
| $H_2O + h\nu \rightarrow H_2O^+ + e^-$ | | *Moses and Bass* [2000] |
| $H^+ + e^- \rightarrow H$ | $1.9 \times 10^{-16} T_e^{-0.7}$ | *Moses and Bass* [2000]; *Kim and Fox* [1994] |
| $H_2^+ + e^- \rightarrow H + H$ | $2.3 \times 10^{-12} T_e^{-0.4}$ | *Moses and Bass* [2000]; *Kim and Fox* [1994] |
| $H_3^+ + e^- \rightarrow H_2 + H$ | $7.6 \times 10^{-13} T_e^{-0.5}$ | *Moses and Bass* [2000]; *Kim and Fox* [1994] |
| $H_3^+ + e^- \rightarrow 3H$ | $9.7 \times 10^{-13} T_e^{-0.5}$ | *Moses and Bass* [2000]; *Kim and Fox* [1994] |
| $He^+ + e^- \rightarrow He$ | $1.9 \times 10^{-16} T_e^{-0.7}$ | *Moses and Bass* [2000]; *Kim and Fox* [1994] |
| $H_2O^+ + e^- \rightarrow O + H_2$ | $3.5 \times 10^{-12} T_e^{-0.5}$ | *Moses and Bass* [2000]; *Miller et al.* [1997] |
| $H_2O^+ + e^- \rightarrow OH + H$ | $2.8 \times 10^{-12} T_e^{-0.5}$ | *Moses and Bass* [2000]; *Miller et al.* [1997] |
| $H_3O^+ + e^- \rightarrow H_2O + H$ | $6.1 \times 10^{-12} T_e^{-0.5}$ | *Moses and Bass* [2000]; *Miller et al.* [1997] |
| $H_3O^+ + e^- \rightarrow OH + 2H$ | $1.1 \times 10^{-11} T_e^{-0.5}$ | *Moses and Bass* [2000]; *Miller et al.* [1997] |
| $H^+ + H_2 \rightarrow H_2^+ + H$ | see text | *Moses and Bass* [2000] |
| $H^+ + H_2 + M \rightarrow H_3^+ + M$ | $3.2 \times 10^{-41}$ | *Moses and Bass* [2000]; *Kim and Fox* [1994] |
| $H^+ + H_2O \rightarrow H_2O^+ + H$ | $8.2 \times 10^{-15}$ | *Moses and Bass* [2000]; *Anicich* [1993] |
| $H_2^+ + H \rightarrow H^+ + H_2$ | $6.4 \times 10^{-16}$ | *Moses and Bass* [2000]; *Anicich* [1993] |
| $H_2^+ + H_2 \rightarrow H_3^+ + H$ | $2.0 \times 10^{-15}$ | *Moses and Bass* [2000]; *Kim and Fox* [1994] |
| $H_2^+ + H_2O \rightarrow H_2O^+ + H_2$ | $3.9 \times 10^{-15}$ | *Moses and Bass* [2000]; *Anicich* [1993] |
| $H_2^+ + H_2O \rightarrow H_3O^+ + H$ | $3.4 \times 10^{-15}$ | *Moses and Bass* [2000]; *Anicich* [1993] |
| $H_3^+ + H_2O \rightarrow H_3O^+ + H_2$ | $5.3 \times 10^{-15}$ | *Moses and Bass* [2000]; *Anicich* [1993] |
| $He^+ + H_2 \rightarrow H^+ + H + He$ | $8.8 \times 10^{-20}$ | *Matcheva et al.* [2001]; *Perry* [1999] |
| $He^+ + H_2 \rightarrow H_2^+ + He$ | $9.4 \times 10^{-21}$ | *Moses and Bass* [2000]; *Kim and Fox* [1994] |
| $He^+ + H_2O \rightarrow H^+ + OH + He$ | $1.9 \times 10^{-16}$ | *Moses and Bass* [2000]; *Anicich* [1993] |
| $He^+ + H_2O \rightarrow H_2O^+ + He$ | $5.5 \times 10^{-17}$ | *Moses and Bass* [2000]; *Anicich* [1993] |
| $H_2O^+ + H_2 \rightarrow H_3O^+ + H$ | $7.6 \times 10^{-16}$ | *Moses and Bass* [2000]; *Anicich* [1993] |
| $H_2O^+ + H_2O \rightarrow H_3O^+ + OH$ | $1.9 \times 10^{-15}$ | *Moses and Bass* [2000]; *Anicich* [1993] |

# 3 dimensional ionospheric model

- Primitive equations
  - Ion

Source and Loss rate

Density: $$\frac{\partial \rho_i}{\partial t} + \frac{1}{A}\frac{\partial (A\rho_i v_{i,\parallel})}{\partial s} = S_i - L_i$$

Momentum: $$\rho_i \frac{\partial v_{i,\parallel}}{\partial t} + \rho_i v_{i,\parallel}\frac{\partial v_{i,\parallel}}{\partial s} = n_i e E_\parallel - \frac{\partial p_i}{\partial s} - \rho_i g - \sum_k \rho_i \nu_{ik}(v_{i,\parallel} - v_{k,\parallel})$$

Temperature: $T_i = T_e$

| | |
|---|---|
| $v_\parallel$ | Field-aligned Velocity |
| $E_\parallel$ | Electric field |
| $A$ | Magnetic flux cross-section |
| $g$ | Gravity and CF |
| $T$ | Temperature |
| $Q$ | Heating rate |
| $\kappa$ | Diffusion coefficient |

$N_i$ ($H^+$, $H_2^+$, $H_3^+$, $He^+$, $H_2O^+$ and $H_3O^+$),

$V_i$ ($H^+$, $H_2^+$, $H_3^+$, $He^+$, [$H_2O^+$, $H_3O^+$ = 0]),

$T_e$, $T_i$

  - Electron

Density: $$n_e = \sum_i n_i$$

Momentum: $$E_\parallel = -\frac{1}{e n_e}\frac{\partial p_e}{\partial s}$$

EUV, collision, Joule heating, photoelectron

Temperature: $$\frac{\partial T_e}{\partial t} - \frac{2}{3}\frac{1}{A}\frac{\partial}{\partial s}\left(A\kappa_e \frac{\partial T_e}{\partial s}\right) = Q_{EUV} + Q_{coll} + Q_{joule} + Q_{ph,ionos}$$

Heat flow, $Q_{HF}$

Heating rate

# Background neutral atmosphere

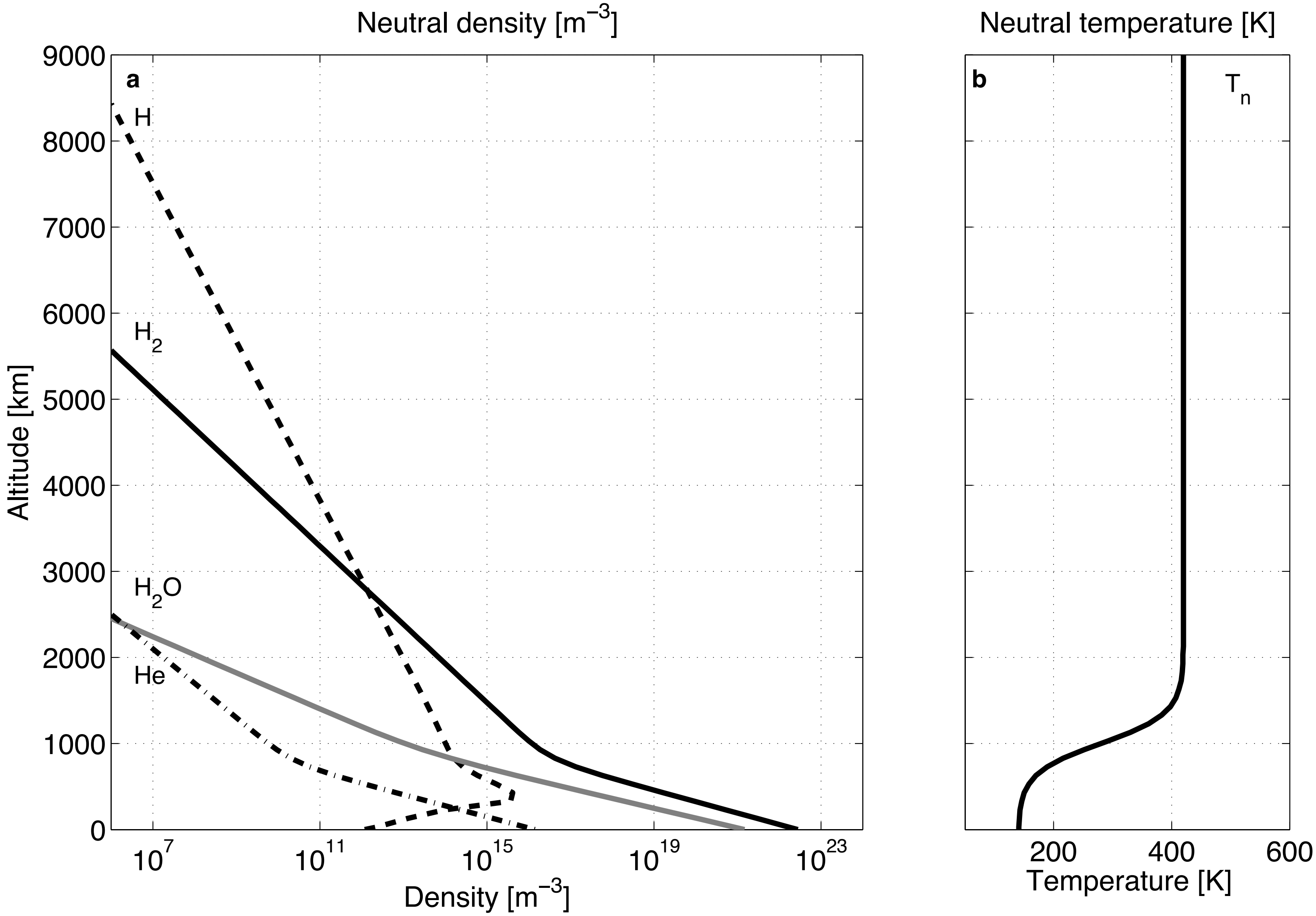

# $N_i$, $V_i$, $\sigma_p$ (L=5, LT=12)

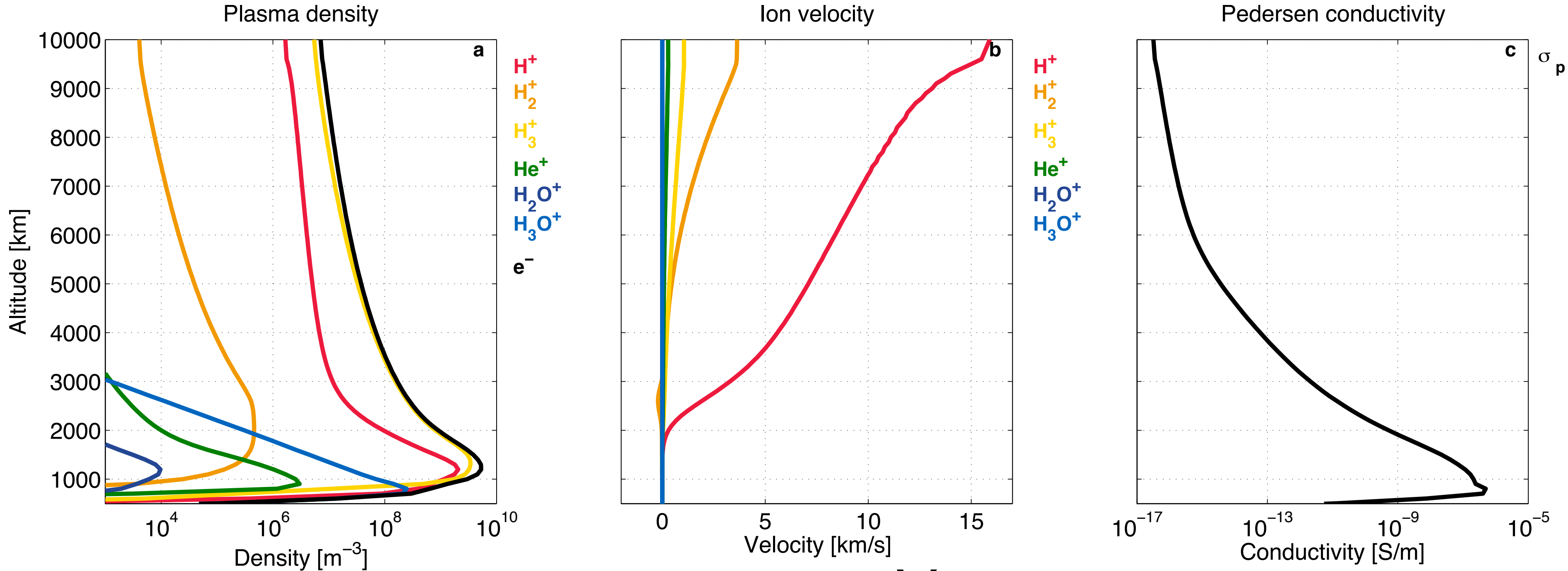


- $N_i$
  - $H_3^+$ is dominant.
    Max: ~$10^{10}$ $m^{-3}$
- $\sigma_i$
  - Maximum around 1000 km
- $V_i$
  - Upward velocity
    - Light component

# $N_i$, $T_e$, $Q_e$ (L=5, LT=12)

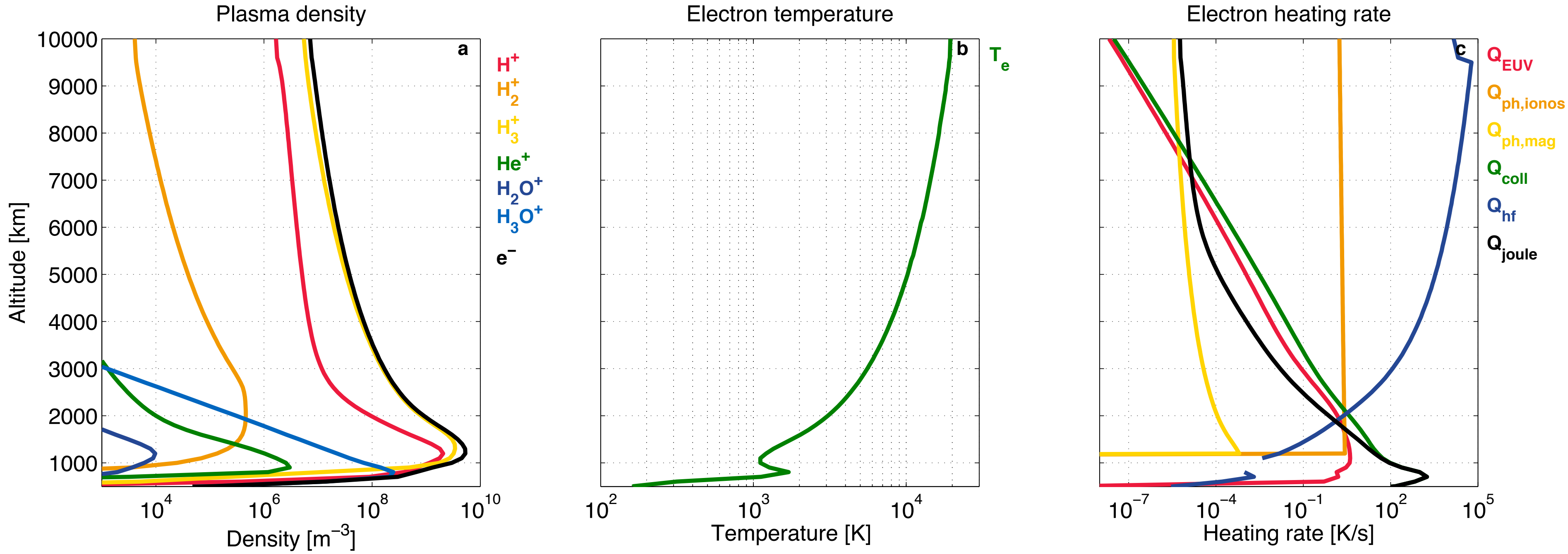


- $T_e$
  - 2000 K at ~1200 km
  - $T_e$ drastically increases.
- Heating rate
  - $Q_{Joule}$ and $Q_{coll}$ are important at low altitude.
  - $Q_{HF}$ is contributing to heat process above topside.

# Diurnal variations of $N_e$, $T_e$ and $\sigma_p$ (L=5)

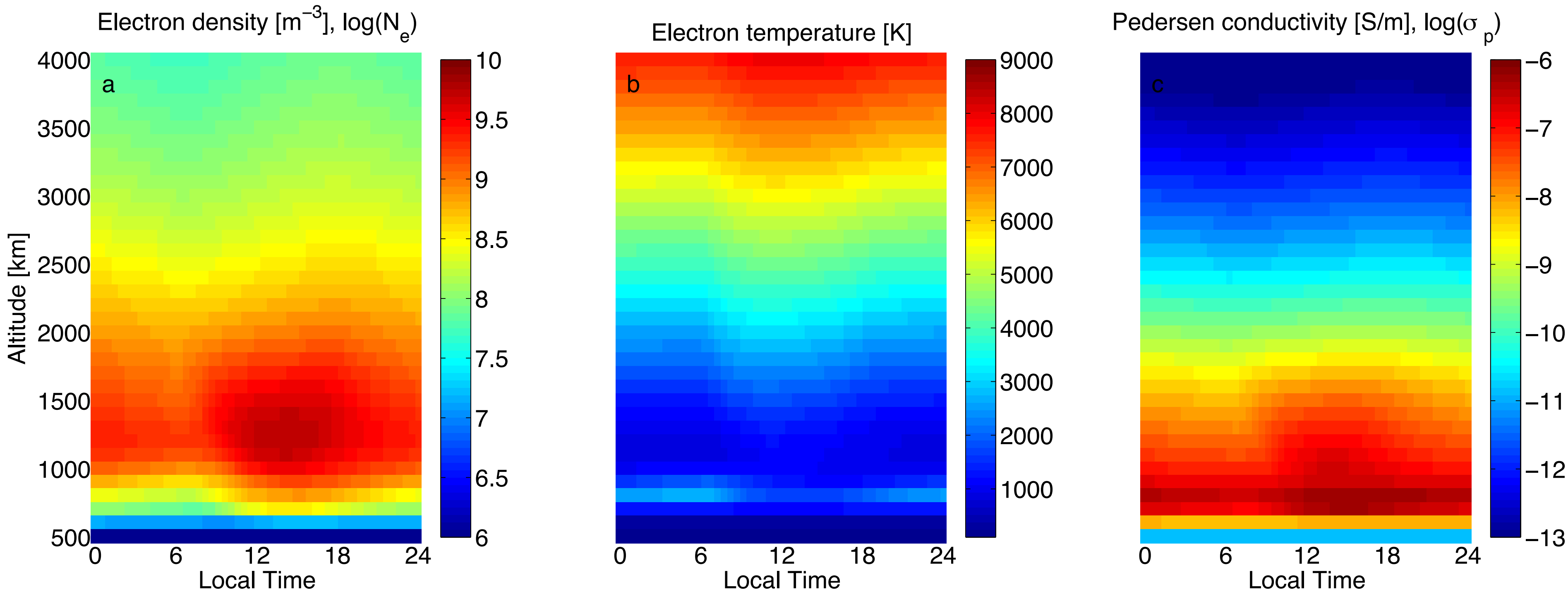


- $N_e$, $\sigma_p$
  - Start to increase after 6 LT
  - Max: ~14 LT
  - $N_e$ and $\sigma_p$ decreases at high altitudes.
- $T_e$
  - Max: ~12 LT
  - $T_e$ is kept to high temperature in all LT by $Q_{HF}$.

# Pedersen conductivity

$$\sigma_p = \sum_i \frac{\nu_i}{\nu_{in}^2 + \omega_{ci}^2} \frac{n_i e^2}{m_i} + \frac{\nu_e}{\nu_{en}^2 + \omega_{ce}^2} \frac{n_e e^2}{m_e}$$

$$\Sigma_i = \int_{z_1}^{z_2} \sigma_p ds$$

- LT dependence of $\sum_i$
- $\sum_i$ decreases with increase of Rs

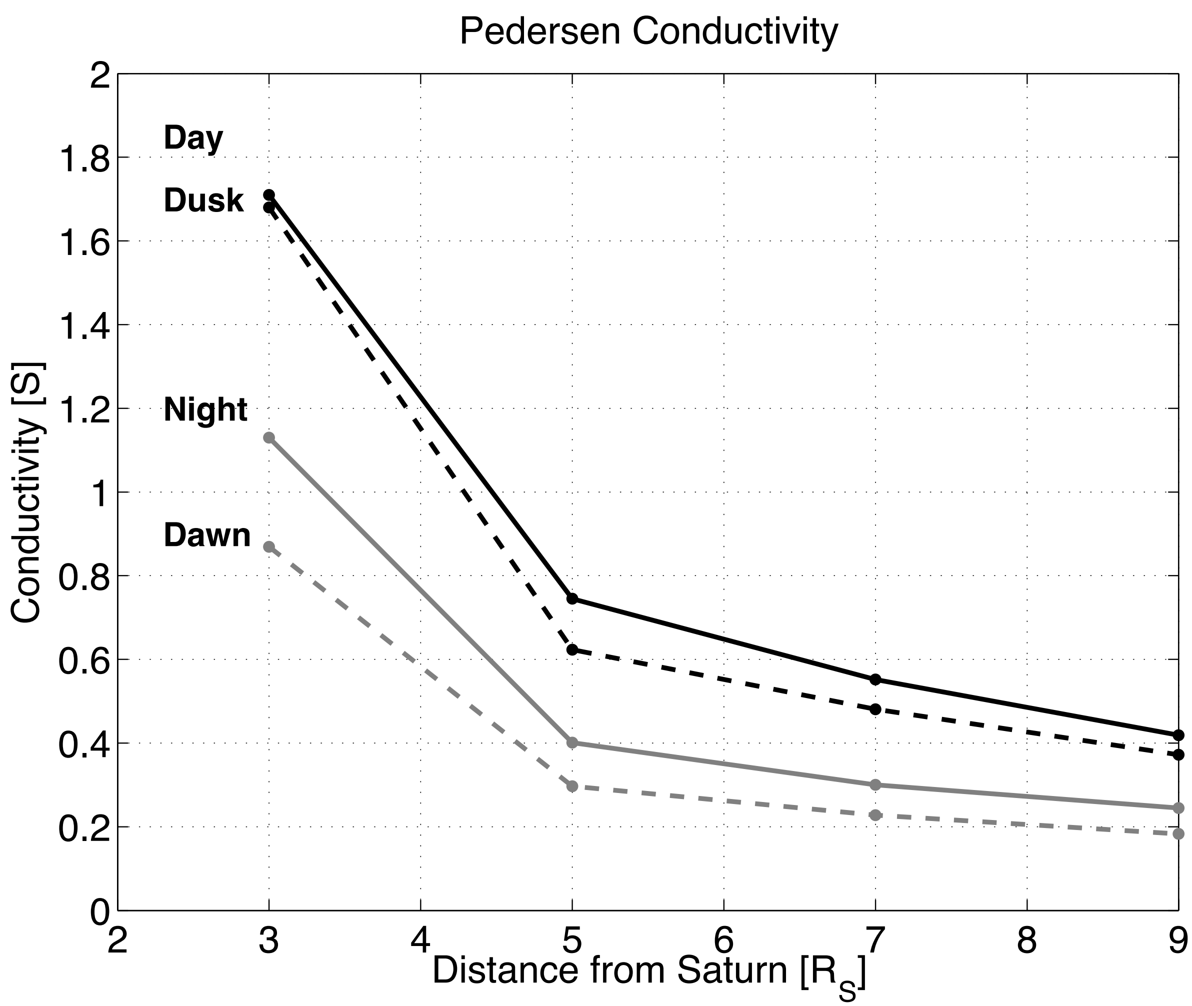

# Magnetospheric ion velocity

1. Modeling of inner magnetosphere with dust-plasma interaction
2. Modeling of ionosphere
3. Magnetosphere-ionosphere coupling

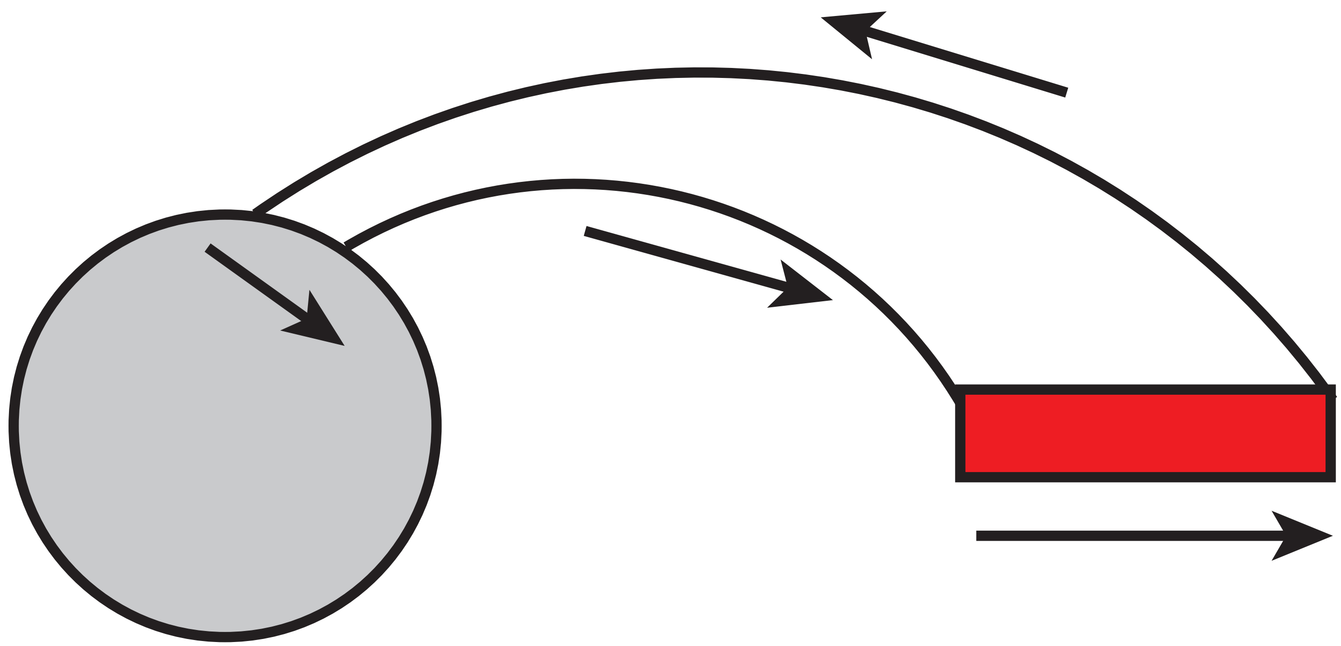

# Magnetospheric ion velocity

1. Modeling of inner magnetosphere with dust-plasma interaction
2. Modeling of ionosphere
3. Magnetosphere-ionosphere coupling

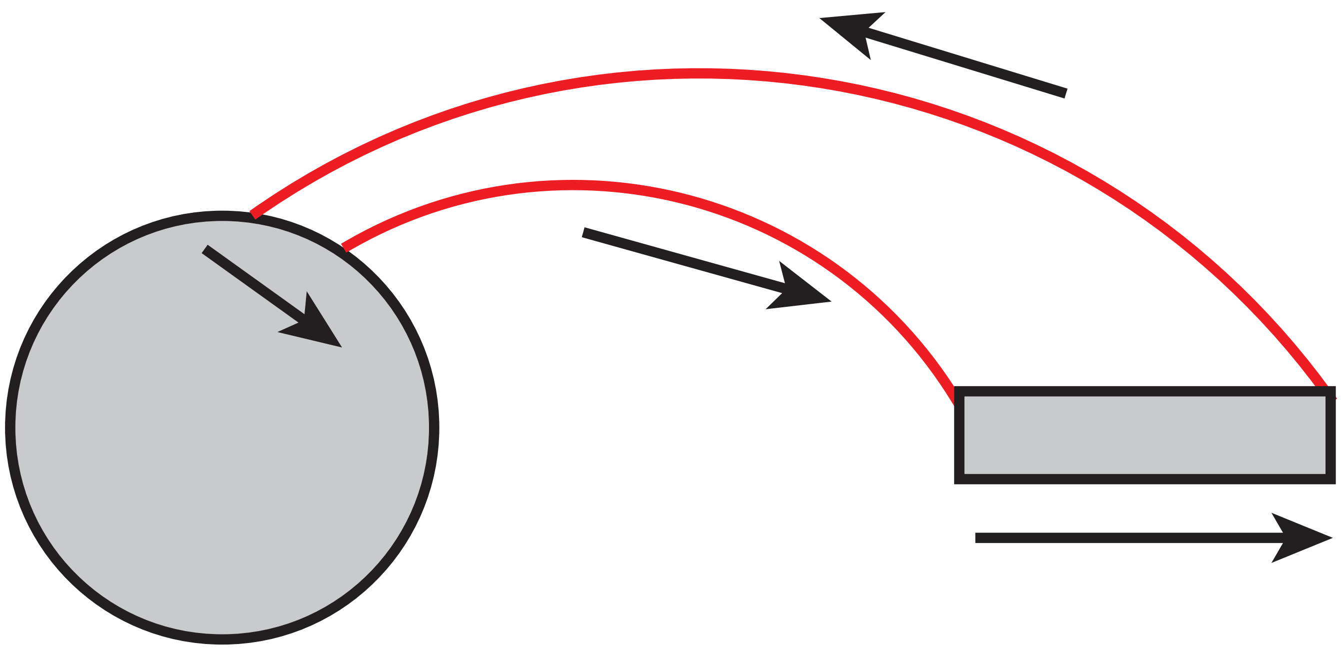

# Magnetospheric ion velocity

1. Modeling of inner magnetosphere with dust-plasma interaction
2. Modeling of ionosphere
3. Magnetosphere-ionosphere coupling

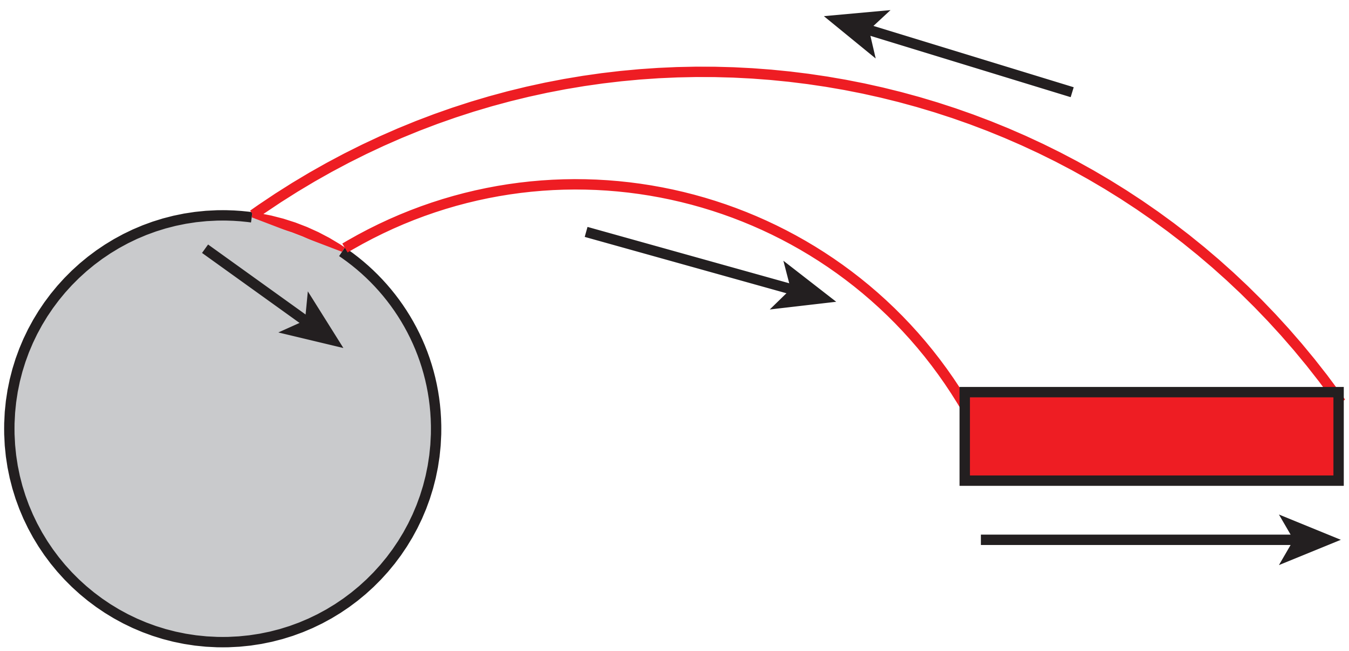

# Magnetospheric ion velocity

$$\Sigma_i \left( \mathbf{E}_{cor} - \mathbf{E} \right) = \mathbf{j} D$$

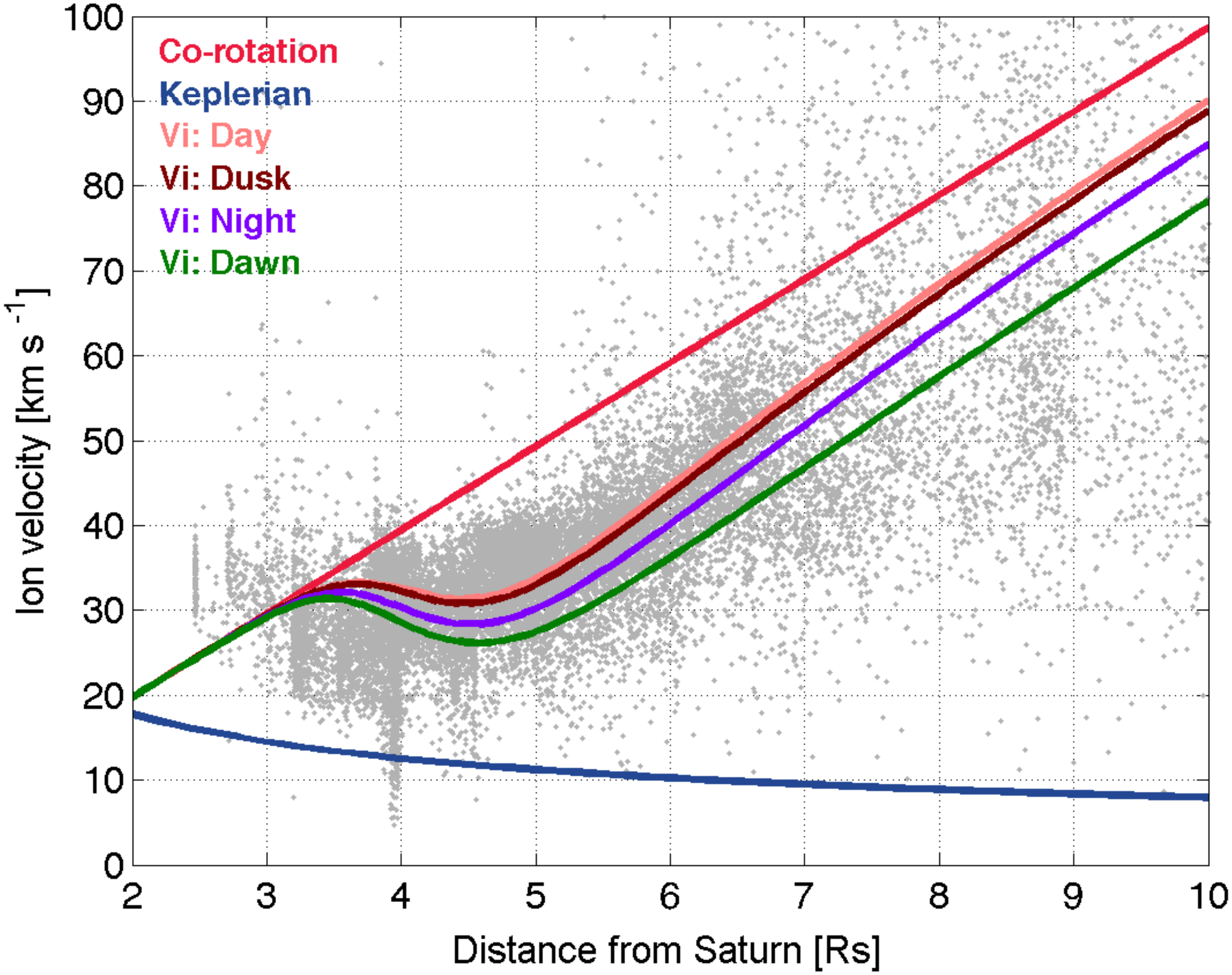


Large dust density, D=1 $R_S$

- $V_i$ depends on LT.

# Summary in ionospheric model

- Ionospheric plasma distribution
  - $H_3^+$ is dominant at L=5.
    - Peak: $10^9$-$10^{10}$ $m^{-3}$
  - $T_e$ is much higher than that of previous studies at high altitude.
    - 2000 K at ~1200 km; 10000 K at ~5000 km
  - Joule heating and collision heating are important at low altitude, and heat flow at high altitude.
- Ionospheric conductivity
  - Pedersen conductivity depends on LT.
    - Day -> Dusk -> Night -> Dawn
  - The magnetospheric ion speed shows the same tendency as the diurnal variation of conductivity.

# Conclusion of this thesis

From Observations

- Inner magnetoshpheric ion speed is slow down from the co-rotation speed.
- Ion speed is Keplerian in the Enceladus plume.

From Modelings

- Ion speed is slow down from the co-rotation speed due to **dust-plasma interaction** and **magnetosphere-ionosphere coupling**.

# Future works

- Improvement of the model:
  - Dust size distribution
  - Charged distribution of dust

# Reference Works


- **Sakai, S.**, S. Watanabe, M. W. Morooka, M. K. G. Holmberg, J. –E. Wahlund, D. A. Gurnett, and W. S. Kurth (2013), Dust-plasma interaction through magnetosphere-ionosphere coupling in Saturn's plasma disk, *Planet. Space Sci.*, *75*, 11-16, doi:10.1016/j.pss.2012.11.003.
- **Sakai, S.**, and S. Watanabe (2014), High-speed flow and high temperature plasma in Saturn's mid-latitude ionosphere, in preparation.
- **Sakai, S.**, M. W. Morooka, J. –E Wahlund, and S. Watanabe (2014), Dusty plasma distribution of Enceladus plume observed by Cassini RPWS/LP, in preparation.